JACS
JOURNAL OF THE AMERICAN CHEMICAL SOCIETY
Article
pubs.acs.org/JACS

The Basis for Carbapenem Hydrolysis by Class A β-Lactamases: A Combined Investigation using Crystallography and Simulations

Fátima Fonseca,*[,†,‡,#] Ewa I. Chudyk,[§] Marc W. van der Kamp,[§] António Correia,[‡] Adrian J. Mulholland,*[,§] and James Spencer*[,†]

[†]School of Cellular and Molecular Medicine, University of Bristol Medical Sciences Building, University Walk, Bristol BS8 1TD, United Kingdom

[‡]CESAM & Department of Biology, University of Aveiro, 3810-193 Aveiro, Portugal

[§]School of Chemistry, University of Bristol, Bristol BS8 1TS, United Kingdom

Supporting Information

ABSTRACT: Carbapenems are the most potent β-lactam antibiotics and key drugs for treating infections by Gram-negative bacteria. In such organisms, β-lactam resistance arises principally from β-lactamase production. Although carbapenems escape the activity of most β-lactamases, due in the class A enzymes to slow deacylation of the covalent acylenzyme intermediate, carbapenem-hydrolyzing class A β-lactamases are now disseminating in clinically relevant bacteria. The reasons why carbapenems are substrates for these enzymes, but inhibit other class A β-lactamases, remain to be fully established. Here, we present crystal structures of the class A carbapenemase SFC-1 from *Serratia fonticola* and of complexes of its Ser70 Ala (Michaelis) and Glu166 Ala (acylenzyme) mutants with the carbapenem meropenem. These are the first crystal structures of carbapenem complexes of a class A carbapenemase. Our data reveal that, in the SFC-1 acylenzyme complex, the meropenem 6α-1R-hydroxyethyl group interacts with Asn132, but not with the deacylating water molecule. Molecular dynamics simulations indicate that this mode of binding occurs in both the Michaelis and acylenzyme complexes of wild-type SFC-1. In carbapenem-inhibited class A β-lactamases, it is proposed that the deacylating water molecule is deactivated by interaction with the carbapenem 6α-1R-hydroxyethyl substituent. Structural comparisons with such enzymes suggest that in SFC-1 subtle repositioning of key residues (Ser70, Ser130, Asn132 and Asn170) enlarges the active site, permitting rotation of the carbapenem 6α-1R-hydroxyethyl group and abolishing this contact. Our data show that SFC-1, and by implication other such carbapenem-hydrolyzing enzymes, uses Asn132 to orient bound carbapenems for efficient deacylation and prevent their interaction with the deacylating water molecule.

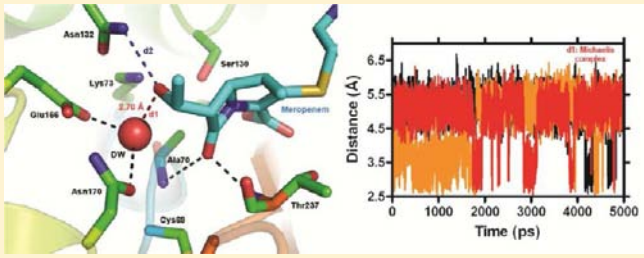

INTRODUCTION

Carbapenems[1,2] are the most recently introduced and potent class of β-lactam antibiotics. These were formerly reserved for severe infections by Gram-negative bacterial pathogens, including both the Enterobacteriaceae (e.g., *Escherichia coli*, *Klebsiella pneumoniae*) and nonfermenting organisms such as *Pseudomonas aeruginosa*, that were unresponsive to other treatments. However, the growth in resistance to alternative agents means that carbapenems are increasingly viewed as front-line therapy for treatment of healthcare-associated infections by both Enterobacteriaceae and nonfermenting pathogens.[3] In these organisms, β-lactam resistance most frequently arises through production of β-lactamases, enzymes that hydrolyze the β-lactam amide bond to abolish its antimicrobial activity.[4] Unsurprisingly, growing carbapenem use has led to an increasing incidence of β-lactamases with carbapenem-hydrolyzing activity.[5,6]

β-lactamases are divided, on the basis of sequence,[7] into four distinct classes: three groups (classes A, C, and D) of serine hydrolases and an unrelated group of zinc metalloenzymes (class B). Carbapenemase activity has now been reported in multiple β-lactamases of classes A, B, and D.[6,8] In the case of the class A serine β-lactamases, several carbapenem-hydrolyzing enzymes (e.g., IMI,[9] NMC,[10,11] SME,[12] KPC,[13] SFC,[14] and certain of the GES enzymes[15−20]) have been identified from a number of environmental and pathogenic organisms. In particular, members of the KPC group are now endemic in Enterobacteriaceae in a number of locations, including the ,Eastern U.S.A., Greece and Israel.[6,21] KPC production results in organisms with reduced susceptibility, or resistance, to carbapenems and for which there are few other effective treatment options.[21] Furthermore, many class A carbapenemases, including KPC, are less sensitive to the mechanism-based inhibitors, such as clavulanic acid, that are effective against the majority of class A β-lactamases.[22]

Received: May 8, 2012
Published: October 3, 2012

Scheme 1. Reaction of Carbapenems with Class A β-Lactamases[a]

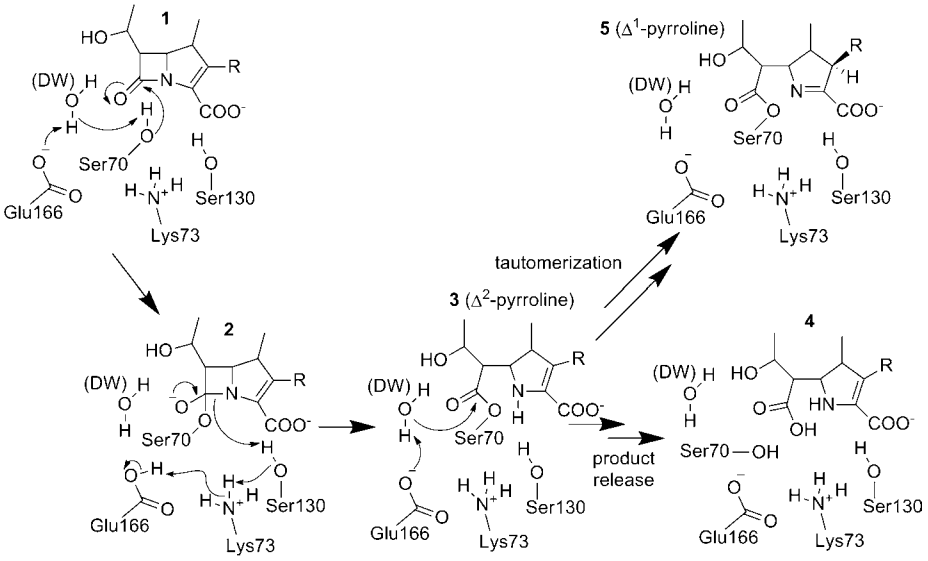

[a]Bound carbapenem in the Michaelis complex (top left; **1**) acylates active-site Ser70 via a tetrahedral intermediate (**2**). Acylenzyme (**3**) in the Δ^2-pyrroline form can resolve to product (**4**; intermediate steps not shown) by nucleophilic attack of the deacylating water molecule (DW) on the acylenzyme carbonyl, or tautomerize to the long-lived Δ^1-pyrroline complex (top right; **5**; intermediate steps not shown). Note the roles of Ser70 amd Glu166 (residues mutated in this study) as nucleophile (**1**) and general base for deacylation (**3**), respectively. Further details and references are given in the text.

Most class A β-lactamases, including widespread and clinically important enzymes such as the TEM, SHV, and CTX-M families,[22] as well as *Mycobacterium tuberculosis* BlaC,[23] are inhibited by carbapenems through formation of a long-lasting acylenzyme complex. Acylation occurs readily by nucleophilic attack of the active site serine Ser70 upon the scissile β-lactam amide bond (Scheme 1; **1**), but the resulting complex (Scheme 1; **3**) deacylates to form product (Scheme 1; **4**), only slowly. Several factors have been proposed to stabilize the carbapenem acylenzyme, including (1) deactivation of the water molecule responsible for deacylation (Scheme 1; DW) by a hydrogen bond to the 6α-1R-hydroxyethyl group of bound carbapenem;[24,25] (2) tautomerization of the acylenzyme from the Δ^2- (Scheme 1; **3**) to the more slowly hydrolyzed Δ^1- (Scheme 1; **5**) pyrroline form (a process facilitated in enzymes such as TEM-1 by donation of a proton from the conserved Arg244[26] or a coordinated water molecule); and (3) displacement of the acylenzyme carbonyl group from the oxyanion hole (formed by the backbone NH groups of Ser70 and Thr237) with consequent destabilization of the transition state for deacylation.[24,25,27,28]

In order to facilitate deacylation of the carbapenem acylenzyme, the interactions of carbapenem-hydrolyzing class A β-lactamases with carbapenems are thus expected to differ substantially from those made by their carbapenem-inhibited counterparts. However, despite multiple structural[29−32] and biochemical[26,33−37] investigations, the basis for carbapenem hydrolysis in these enzymes remains to be fully established. Although carbapenemase activity has been associated with the presence of a disulfide bond between Cys69 and Cys238[34] and/or the absence of Arg at position 244,[26] these features alone are insufficient for high-level carbapenemase activity. Several crystal structures reveal that the active sites of class A carbapenenases closely resemble those of carbapenem-inhibited enzymes. Together, the absence of conserved structural features that distinguish carbapenemases, and the overall homology between the active sites of carbapenem-hydrolyzing and carbapenem-inhibited enzymes, suggest that multiple subtle alterations, rather than gross distortions of the active site, may collectively be responsible for activity against carbapenem substrates.[30,35] Importantly, however, the interactions between class A carbapenemases and their carbapenem substrates remain to be structurally characterized.

SFC-1 is a class A β-lactamase identified from strain UTAD54 of the environmental Gram-negative bacterium *Serratia fonticola*, an occasional opportunist pathogen responsible for respiratory tract and wound infections.[38] Unusually, *S. fonticola* UTAD54 contains two carbapenem-hydrolyzing β-lactamases, SFC-1[14,39] and a class B metallo-β-lactamase Sfh-I.[40−42] SFC-1 is a potent carbapenemase that also hydrolyzes extended-spectrum cephalosporins and shows reduced susceptibility to mechanism-based inhibitors such as clavulanic acid[39]—thus sharing many of the characteristics of the widely distributed KPC enzymes[13,21,43,44] with which it has 69% sequence identity. As SFC-1 is thus an appropriate model system in which to study carbapenem-hydrolyzing class A β-lactamases, and the molecular basis of carbapenemase activity in such enzymes remains to be fully elucidated, we have determined the crystal structure of SFC-1 and two site-directed mutants that enabled us to trap Michaelis and acylenzyme complexes with the carbapenem meropenem (Figure 1). To our knowledge, these are the first structures to be reported for stabilized carbapenem complexes of a carbapenem-hydrolyzing class A β-lactamase. These data, together with the results of

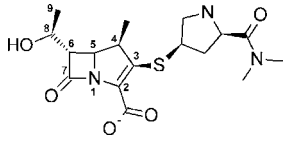

Figure 1. Meropenem (carbapenem used in this study).

dx.doi.org/10.1021/ja304460j | J. Am. Chem. Soc. 2012, 134, 18275−18285

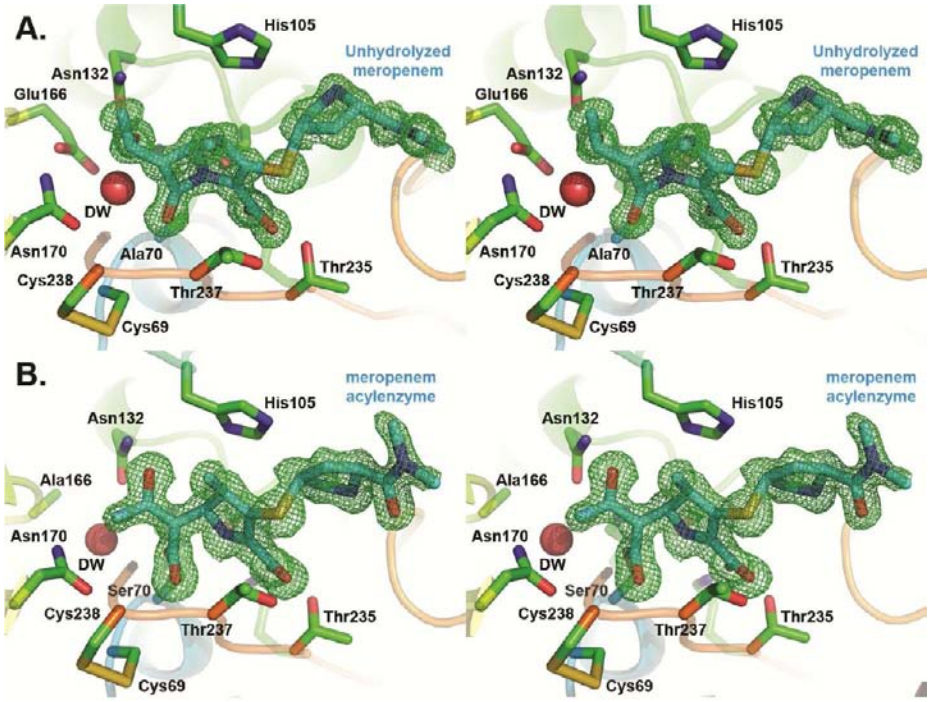

Figure 2. Meropenem complexes of SFC-1 mutants. Stereoviews of (A) Michaelis complex (Ser70 Ala mutant) and (B) acylenzyme complex (Glu166 Ala mutant). C_α atoms color ramped from blue (N) to red (C) termini. Otherwise, atom colors as standard, except carbon atoms in green (protein) or cyan (ligand). Electron density maps shown are $|F_o| - |F_c|.\phi_{calc}$, contoured at 3.0 σ about the bound ligand (positive density; green). Phases were calculated from models from which ligands were omitted. This figure and Figures 3, 4, 6, and 7 were created using PyMOL (www.pymol.org).

molecular dynamics (MD) simulations on the wild-type enzyme, reveal how SFC-1, and by implication other class A carbapenemases, binds and reacts with carbapenems in a fashion consistent with efficient deacylation, and how the interactions required for this transformation differ from those made by other class A β-lactamases against which carbapenems are effective inhibitors.

MATERIALS AND METHODS

General. General reagents were purchased from Sigma, Merck, or Acros Organics and were of analytical grade. Crystallization reagents and consumables were purchased from Hampton Research or Molecular Dimensions.

Directed Mutagenesis, Expression, and Protein Purification. *S. fonticola* UTAD54 SFC-1 was expressed in the T7 vector pET-26(b) (Novagen) as previously described.[39] This plasmid was used as a template for site-directed mutagenesis performed using the QuikChange Mutagenesis kit (Agilent) according to the manufacturer's protocols. Sequences of the mutagenic oligonucleotide primers used are provided in Supporting Information (Table S1). Plasmids were purified from recombinant colonies (QIAprep spin; QIAGEN) obtained at the end of the Quikchange procedure and the complete SFC-1 open reading frame sequenced on both strands (The Sequencing Service, University of Dundee, U.K.) to verify introduction of the desired mutation. (Our sequencing revealed two amino acid differences between SFC-1 as previously kinetically characterized[39] and used in the structural studies described here, and the sequence as originally deposited.[14] Both of these are at positions remote from the active site). Wild-type and mutant plasmids were transformed into *E. coli* strain BL21 (DE3) (Novagen). Overexpression and purification of the wild-type and mutant proteins were performed as described for wild-type SFC-1.[39]

Crystallization. Diffraction quality (1.38 Å resolution; SI Table S2) single crystals of wild-type SFC-1 were grown at 20 °C by hanging drop vapor diffusion mixing 1.5 μL of protein (30 mg/mL in 10 mM sodium phosphate pH 7.0) with 1.5 μL of reservoir solution and equilibrating the samples against 500 μL of reservoir solution. The reservoir solution contained 18−22% w/v poly(ethylene glycol) 3350, 0.2 M sodium acetate (unbuffered). Crystals of SFC-1 mutants (30 mg/mL protein; 1.08 Å resolution (Ser70 Ala); 1.30 Å resolution (Glu166 Ala)) were obtained by seeding using crystals of the wild-type protein and the same reservoir solution. The crystals used for data collection were cryo-cooled in liquid nitrogen using reservoir solution supplemented with 20% ethylene glycol as cryoprotectant.

Complexes were prepared by soaking crystals of the mutant proteins, SFC-1 Ser70 Ala (expected to stabilize the Michaelis complex as Ser70 is the nucleophile essential for acylation[4,45]) and SFC-1 Glu166 Ala (expected to stabilize the transient acylenzyme complex as Glu166 activates the water molecule required for deacylation[4,45−47]) in cryoprotectant solution containing 50 mM meropenem for 30 to 50 min prior to snap-freezing in liquid nitrogen.

X-ray Diffraction Data Collection, Structure Solution, and Refinement. Diffraction data were collected at 100 K on ADSC Quantum series CCD detectors mounted on beamlines 10.1 of the Synchrotron Radiation Source (Daresbury, UK; wild-type enzyme) and IO2/IO3 of the Diamond Light Source (Didcot, UK; mutant proteins). Diffraction data were integrated and scaled using the programs HKL2000[48] or MOSFLM[49] and SCALA[50] as shown in SI Table S2. Structures were solved by molecular replacement with PHASER[51] using chain A of *K. pneumoniae* KPC-2 (PDB ID 2OV5;[30] wild-type SFC-1) or the wild-type SFC-1 structure (mutant proteins) as the initial search model. Model building and refinement were performed with the programs COOT[52] and REFMAC,[53] respectively. The models were further refined using conjugate gradient minimization in SHELXL.[54] The progress of crystallographic refinement was monitored using MOLPROBITY[55] and the quality of the final structures was verified with PROCHECK.[56] Data collection and refinement statistics are summarized in SI Table S2.

Molecular Dynamics. The starting structures for simulations were taken from the crystallographic study. Ala70 (for the Michaelis complex) and Ala166 (for the acylenzyme) were mutated back to the

dx.doi.org/10.1021/ja304460j | J. Am. Chem. Soc. 2012, 134, 18275−18285

wild-type residues in silico, based on the conformations present in the other structures. Protonation states and His tautomers were determined using the H++ server (http://biophysics.cs.vt.edu/). The AMBER 11 package[57] with the AMBER ff99SB force field[58] (protein) or the General Amber Force Field[59] (ligand) was used. Partial charges for the free and covalently bound ligand were obtained by RESP fitting of HF/6-31G* calculations performed using *Gaussian09* and RED-IV through the RED Server (http://q4md-forcefieldtools.org/REDS/). Simulations were performed for three different systems: the apoenzyme, the Michaelis complex, and the acylenzyme. Each system was solvated in a rectangular box of TIP3P water molecules extending at least 10 Å from any protein atom and chloride ions were added to neutralize the system. The systems were prepared for production simulation under constant temperature and pressure using a five-step protocol including minimization, heating, and restrained and unrestrained dynamics (details in Supporting Information). Thereafter, production simulations were run for 5 ns at 300 K and 1 atm. The AMBER program ptraj was used for analysis of the MD results. Each simulation was run three times with different starting velocities to confirm the reproducibility of the observed results.

RESULTS

X-ray Crystal Structures of SFC-1. The crystal structure of wild-type SFC-1 was readily determined by molecular replacement using KPC-2[30] as a search model. The SFC-1 overall fold (Figure S1; see Supporting Information for a full description of the wild-type structure) closely resembles those of both carbapenem-hydrolyzing and carbapenem-inhibited class A β-lactamases (SI Figure S2). This is consistent with previous conclusions[30,35] that multiple subtle alterations to the active site are required for efficient carbapenemase activity in these enzymes. In addition to a molecule of ethylene glycol (present in the crystallization buffer as a cryoprotectant), the SFC-1 active site (SI Figure S3) contains two water molecules. One of these, the presumed deacylating water molecule, DW, is appropriately positioned, close to Ser70, to participate in both the acylation and deacylation steps of the reaction (Scheme 1) and is hydrogen-bonded to the Nδ2 or Oδ1 atoms of Asn170 (present in two conformations) and Glu166 Oε2. The second, OW, occupies the oxyanion hole formed by the backbone nitrogen atoms of Ser70 and Thr237 (SI Figure S3).

In order to better understand the basis for carbapenemase activity in Class A β-lactamases, we sought to reveal the interactions of such enzymes with these substrates by determining structures of carbapenem complexes of SFC-1. Attempts to obtain complex structures by soaking crystals of the wild-type enzyme were unsuccessful, most likely due to the high catalytic activity of SFC-1 toward the carbapenem tested (meropenem; Figure 1). Accordingly, we constructed acylation- (Ser70 Ala) and deacylation- (Glu166 Ala) deficient mutants to facilitate trapping of complexes. Mutation of the serine nucleophile (Scheme 1) has previously been used to trap complexes of the Class A CTX-M[60] and Class C AmpC β-lactamases with unhydrolyzed substrate,[61] while mutants of the Glu166 general base (Scheme 1) have enabled crystal structures to be determined for a variety of acylenzymes of Class A β-lactamases.[45,62,63] This approach enabled us to resolve clear electron density for unhydrolyzed meropenem bound to SFC-1 Ser70 Ala, and for the acylenzyme intermediate bound to SFC-1 Glu166 Ala at close to atomic resolution (Figure 2A,B).

Meropenem Complexes of SFC-1. SFC-1 Ser70 Ala binds unhydrolyzed meropenem in a single well-defined orientation in which the complete meropenem molecule, including the entire C3 substituent, is clearly resolved (Figure 2A). Compared to the wild-type structure, only minimal overall conformational change occurs on binding substrate (Cα rmsd 0.47 Å). The β-lactam carbonyl displaces the OW water molecule to occupy the oxyanion hole and the C2 carboxylate forms hydrogen bonds to Oγ of Ser130 and Nζ of Lys234 (Oδ1) and to the side-chain hydroxyls of Thr235 and Thr237 (Oδ2; Figure 3A). Importantly, the C8 hydroxyl group of the meropenem 6α-1R-hydroxyethyl substituent makes good hydrogen-bonds with both the putative deacylating water (DW) (2.70 Å; Figure 3A distance d1) and Nδ2 of Asn132 (2.95 Å; Figure 3A distance d2). In addition, a single conformation is now observed for Asn170, which makes hydrogen bonds to both Glu166 and the deacylating water (DW).

Many of these features are preserved in the structure of the acylenzyme formed on reaction of the Glu166 Ala mutant with meropenem (Figure 2B). Bound meropenem occupies a single well-defined conformation, with experimental electron density clearly locating the entire C3 substituent (Figure 2). The planar geometry at C3 (i.e., sp_2 hybridization) unambiguously confirms that the observed acylenzyme is in the Δ^1 tautomer. Consistent with our observations for the Ser70 Ala Michaelis complex, the C2 carboxylate makes hydrogen bond contacts to Lys234 Nζ, Thr235 Oδ1 and Thr237 Oδ1 and the acylenzyme carbonyl group remains positioned in the oxyanion hole. However, we also observe significant differences between the two complex structures. Notably, the meropenem 6α-1R-hydroxyethyl group is rotated by approximately 120° compared to its orientation in the Michaelis complex, such that while a hydrogen-bond between the C8 hydroxyl and Asn132 Nδ2 (Figure 3B, distance d2, 2.87 Å) is retained, that with the deacylating water molecule DW is lost (Figure 3B, distance d1, 4.97 Å). Despite the absence of Glu166, a putative deacylating water molecule (DW) is still present, but its position is shifted by 1.85 Å relative to that in the Ser70 Ala (Michaelis) and by 2.36 Å relative to that in the wild-type enzyme. This water molecule (DW) makes hydrogen bonds to the Oδ1 atom of Asn132 (2.99 Å) and to the main chain carbonyl of Ala166 (2.77 Å; Figure 3B). The latter interaction is made possible by a local reorientation of the protein backbone around position 166 (Cα - Cα distance 1.29 Å for residue 166; rmsd 0.48 Å for the complete polypeptide), compared to the wild-type structure.

MD Simulations of meropenem Complexes of Wild-Type SFC-1. The crystal structures define the positions of bound meropenem in the SFC-1 active site in the unhydrolyzed and acylenzyme states. However, the possibility remains that the mutations required to trap these species for crystallographic observation affect the conformations adopted by bound meropenem. We therefore used molecular dynamics (MD) simulations to investigate the orientation of meropenem in Michaelis and acylenzyme complexes of wild-type SFC-1 in silico. Ser70 and Glu166 were introduced into the experimentally determined Michaelis and acylenzyme complexes and the resulting structures subjected to (three 5 ns) MD simulations. Both sets of simulations were stable, as judged by the time dependence of backbone (Cα) rmsd values (with respect to the relevant crystal structures; Figure S4) and the lack of significant deviation between representative MD models (generated by performing clustering analysis on the final 2.5 ns of these simulations) and the experimentally determined crystal structures (Figure S5). Importantly, this analysis also confirms that the overall orientation of bound meropenem is not grossly affected by the mutations at amino acids 70 or 166 (Figure 4). The positions of the β-lactam and dihydropyrrole rings remain

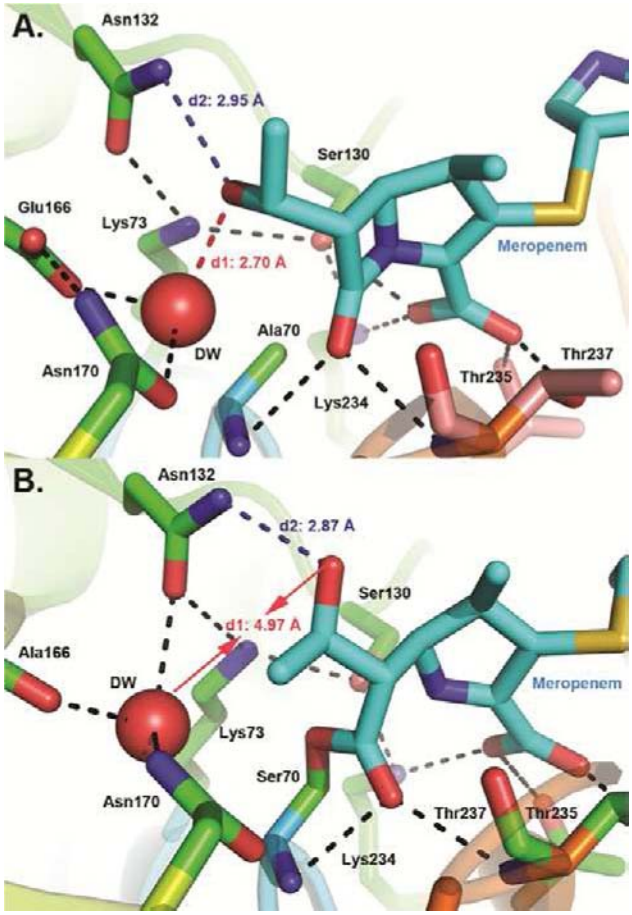

Figure 3. Environment of the deacylating water molecule (DW) in SFC-1:meropenem complexes. (A) Michaelis complex (Ser70 Ala mutant). (B) acylenzyme complex (Glu166 Ala mutant). Cα atoms are color ramped from blue (N) to red (C) termini. Otherwise, atom colors as standard, except carbon atoms in green (protein) or cyan (ligand). Deacylating water (DW) is shown as a red sphere. Hydrogen bonds are shown as dashed lines. H-bonds between the meropenem 6α-1R-hydroxyethyl group and the deacylating water (DW) and Asn132 Nδ2 are shown as red and blue dashed lines, respectively.

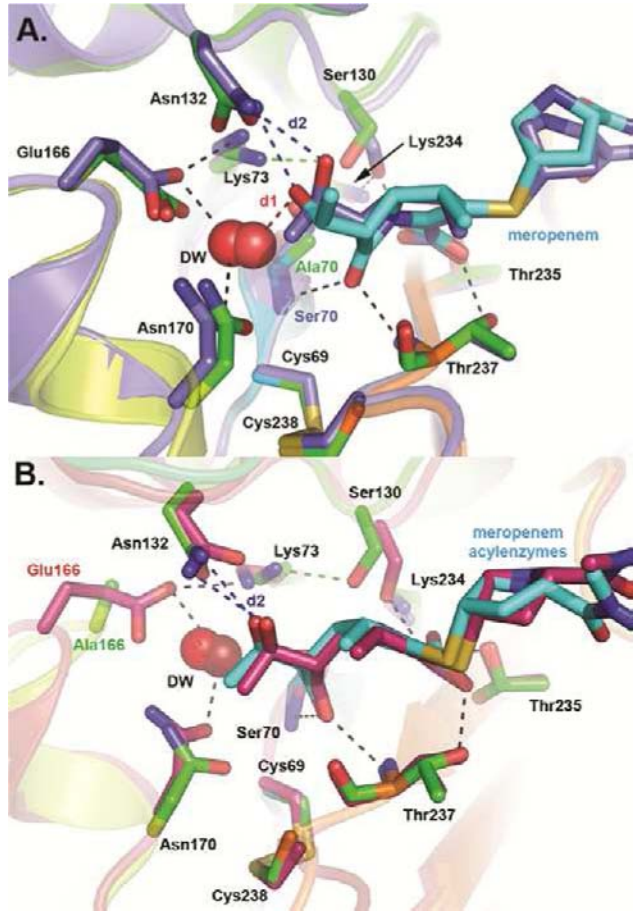

Figure 4. Comparison of crystal structures with MD simulations for SFC-1:meropenem complexes: Comparison of experimental crystal structures with models obtained by clustering analysis of the final 2.5 ns of simulation for three MD trajectories each of the wild-type SFC-1 Michaelis and acylenzyme complexes. (A) Active site of SFC-1 Ser70 Ala structure overlaid on MD model for the wild-type Michaelis complex. (B) Active site of SFC-1 Glu166 Ala structure overlaid on MD model for the wild-type acylenzyme complex. Protein chains are color-ramped from blue (N) to red (C) termini (experimental crystal structures) or colored blue (wt Michaelis complex model) or red (wt acylenzyme complex model). Carbon atoms of ligands and side chains of selected active site residues are shown in cyan and green, respectively (experimental structures); blue (MD model of Michaelis complex) or red (MD model of acylenzyme complex). Atom colors are otherwise as standard. Hydrogen bonds are rendered as dashed lines. Those involving the meropenem 6α-1R-hydroxyethyl group are shown for both experimental and MD structures; the Ser130 Oγ:Lys73 Nζ bond observed in the crystal structures is shown in green. Other H-bonds are shown for the MD models only; colors are as above (Figure 3).

stable, and key interactions, such as those of the meropenem carbonyl with the SFC-1 oxyanion hole and C2 carboxylate with the side chain hydroxyls of Ser130, Thr235, and Thr237, are retained throughout the simulation.

Some small, but significant, differences are, however, evident from close comparison of the results of clustering analysis of our MD simulations with the experimental crystal structures. First, addition of Glu166 to the acylenzyme structure leads to a repositioning of the protein backbone to enable interaction of the deacylating water DW with the Glu166 side chain, rather than the backbone carbonyl group. In the representative structure from MD, the Cα of Glu166 is displaced 2.19 Å, 0.92 Å, and 0.91 Å away from the Cα atoms of Ala166, Glu166, and Glu166 in the acylenzyme, wild-type (apo), and Ser70 Ala (Michaelis complex) crystal structures, respectively. Second, in the simulations of both the Michaelis and acylenzyme complexes, the interactions made by the side chains of the active site residues Lys73, Ser130, Asn132, and Glu166 differ from those observed in the crystal structures (Figure 4). In all three crystal structures reported here, Ser130 Oγ is hydrogen-bonded to Lys73 Nζ (distances between 2.79 Å (acylenzyme) and 3.36 Å (wild-type; Figure 4, green dashed lines)). In the simulations, Ser130 Oγ interacts predominantly with Lys234 Nζ, and the C2 carboxylate of bound meropenem, and contact with Lys73 is lost. The side chain of Lys73 repositions, compared to the experimentally determined crystal structures, to bring it closer to Glu166 (the Lys73 Nζ:Glu166 Oε2 distance is reduced from 3.16 Å in the Michaelis complex crystal structure to 2.74 Å in the representative structure from MD; Figure 4A). In the MD simulations of the acylenzyme complex, Lys73 Nζ and Glu166 Oε2 are within 3.0 Å of one another for over 96% of the total duration.

Previous QM/MM studies of both the acylation[64] and deacylation[47] steps of the reaction of the benzylpenicillin-

dx.doi.org/10.1021/ja304460j | J. Am. Chem. Soc. 2012, 134, 18275−18285

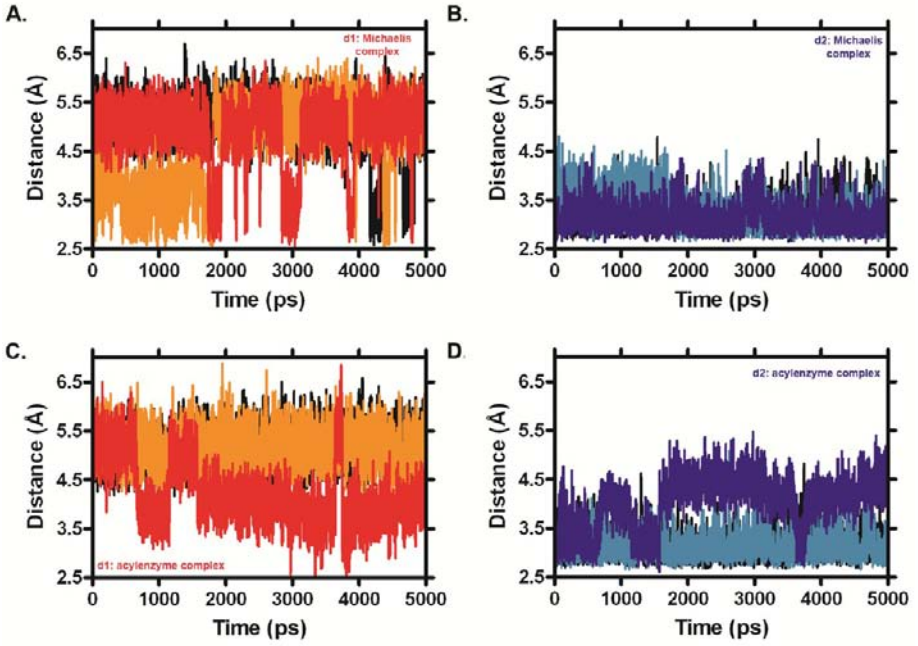

Figure 5. Variation in distances between selected active site atoms over the course of 5 ns MD simulations. (A) meropenem hydroxyethyl OH − deacylating water (DW) for simulations of the Michaelis complex (Figure 3A, d1). (B) meropenem hydroxyethyl OH − Asn132 Nδ1 for simulations of the Michaelis complex (Figure 3A, d2). (C) meropenem hydroxyethyl OH − deacylating water (DW) for simulations of the acylenzyme complex (Figure 3B, d1). (D) meropenem hydroxyethyl OH − Asn132 Nδ1 for simulations of the acylenzyme complex (Figure 3B, d2). Results for three independent simulations are shown in red, orange, and black (panels A,C) and blue, cyan, and black (panels B,D), respectively.

hydrolyzing class A β-lactamase TEM-1 indicate a close contact between the general base Glu166 and Lys73 (important for transition state stabilization and proton transfer;[47,64,65] Scheme 1) in both the Michaelis complex and the acylenzyme. In contrast, in crystal structures of β-lactam complexes of Class A β-lactamases (obtained using either poor substrates or, as here, catalytically impaired mutants) this interaction may be weakened or absent altogether. (For example, Lys73 Nζ and Glu166 Oε2 are 4.09 Å apart in the SHV-1:meropenem complex.[24]) The persistent interaction between Lys73 and Glu166, observed in MD simulations of both the wild-type Michaelis and acylenzyme complexes (Figure 4), thus leads us to consider that our simulations represent catalytically competent conformations.

The MD simulations also reveal significant flexibility in the interactions of the meropenem 6α-1R-hydroxyethyl group with the SFC-1 active site in the wild-type Michaelis complex. For the Michaelis complex, the time-dependence of the meropenem C8 OH:DW distance (d1; Figure 5A), reveals significant movement of these two groups relative to one another such that they are not in hydrogen-bonding contact (d1 > 4.5 Å) for the majority of the duration of the three MD runs performed. However, for the same simulations, the meropenem OH: Asn132 Nδ2 distance (d2; Figure 5B) is shorter and less variable, suggesting that interaction between these two groups is retained. Taking into consideration the representative structure from the latter portion of the MD runs (Figure 4A and SI Figure S5A), these data indicate that, in the Michaelis complex formed by wild-type SFC-1 with meropenem, the meropenem C8 hydroxyl is able to rotate away from the position adopted in the crystal structure (hydrogen bonded to the deacylating water DW and to Asn132 Nδ2) to a conformation resembling that found in the experimental acylenzyme complex (hydrogen-bonded to Asn132 Nδ2, but not to DW; Figure 4A). The time dependence of distance d1 (Figure 5A) indicates that the meropenem 6α-1R-hydroxyethyl group "flips" between positions approximating those in the Michaelis and acylenzyme complexes. Importantly, for the majority of the MD simulation, the 6α-1R-hydroxyethyl group is not in close contact with the deacylating water. Thus, for the Michaelis complex with wild-type SFC-1, the rotated orientation of the 6α-1R-hydroxyethyl group observed in the experimental acylenzyme complex structure is the most likely stable conformation. Our observation of the less favored conformer in the Ser70 Ala (Michaelis complex) crystal structure might then arise from repositioning of the deacylating water, in the absence of Ser70, to a location where a stronger hydrogen bond to the meropenem 6α-1R-hydroxyethyl group is possible than is the case in the wild-type enzyme.

Some variability is also observed in the interactions made by the meropenem 6α-1R-hydroxyethyl group during simulations of the wild-type acylenzyme complex. However, taken across the three MD runs, the meropenem C8 hydroxyl group spends the majority of the simulations relatively distant from the deacylating water DW (distance d1 > 4.5 Å; Figure 5C) while remaining close to Asn132 Nδ2 (distance d2 < 3.75 Å; Figure 5D). Overall, the representative structure of the wild-type acylenzyme from simulation closely resembles the experimentally observed crystal structure of the Glu166 Ala acylenzyme (Figure 4B and SI Figure S5B). Our simulations thus suggest that our Glu166 Ala crystal structure also describes the favored orientation of the meropenem 6α-1R-hydroxyethyl group in the wild-type acylenzyme complex.

■ DISCUSSION

Despite the growing reliance on carbapenem antibiotics for treatment of opportunist infections by Gram-negative bacteria, and the increasing prevalence of carbapenem-hydrolyzing β-

dx.doi.org/10.1021/ja304460j | J. Am. Chem. Soc. 2012, 134, 18275−18285

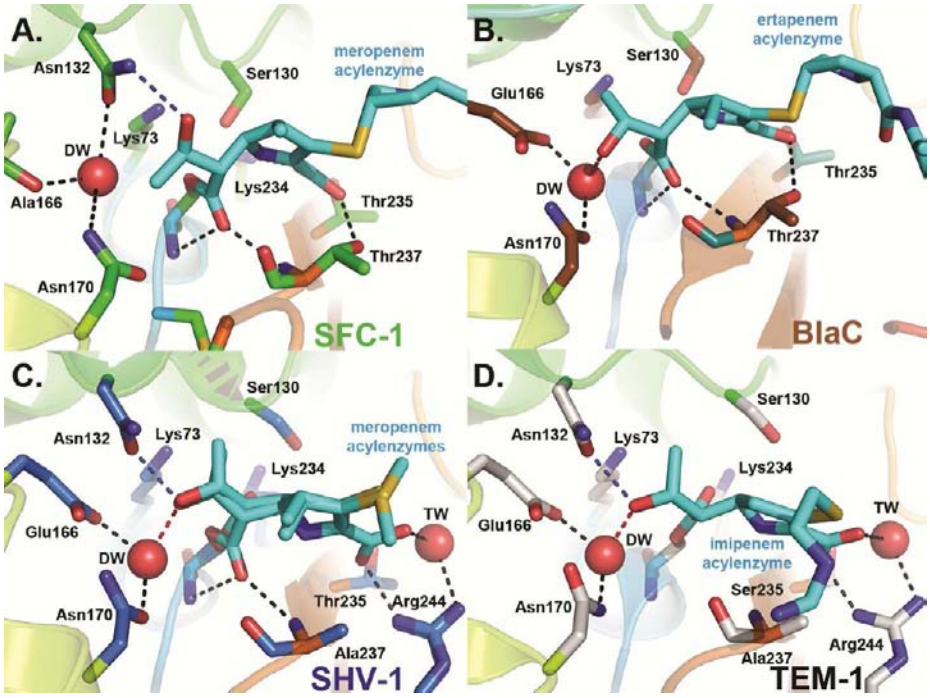

Figure 6. Comparison of carbapenem acylenzymes of class A β-lactamases. (a) SFC-1 Glu166 Ala:meropenem acylenzyme (PDB accession 4EV4); (b) BlaC:ertapenem (Δ^2-pyrroline, 3M6B[68]); (c) SHV-1:meropenem (2ZD8[24]); (d) TEM-1:imipenem (1BT5[25]). In all panels, Cα atoms are color-ramped from blue (N) to red (C) termini and carbapenem carbon atoms are rendered in cyan. Selected active site residues are shown in stick mode with carbon atoms green (SFC-1), brown (BlaC), blue (SHV-1), or gray (TEM-1). Atom colors are otherwise standard. Hydrogen bonds involving the deacylating water molecule (red sphere, DW), the acylenzyme carbonyl group, and the carbapenem C2 carboxylate are indicated by dashed lines with the interactions between the carbapanem 6α-1R-hydroxyethyl group and DW (d1) and Asn132 ND2 (d2) shown in red and blue, respectively. The water molecule involved in tautomerization of the SHV-1 and TEM-1 acylenzymes (TW) is shown as a red sphere. Note that, as Asn132 is replaced by Gly in BlaC, no side chain at this position is shown in panel B.

lactamases, the molecular basis for carbapenem hydrolysis in the class A enzymes has remained elusive. Although the Protein Data Bank (PDB) contains multiple crystal structures of class A β-lactamases with carbapenemase activity,[29−32] structures of these enzymes in complex with carbapenem substrates have so far not been available. Our determination of high-resolution crystal structures for meropenem complexes of SFC-1 thus provides new information on how a subset of class A β-lactamases efficiently hydrolyze carbapenems, rather than forming stable acylenzyme complexes that are resistant to deacylation.

Identification of structural features likely to contribute to the carbapenemase activity of SFC-1 (and by implication related carbapenem-hydrolyzing class A β-lactamases) is greatly facilitated by comparison with equivalent complexes for carbapenem-inhibited enzymes. Recently, a high-resolution structure was determined for the meropenem acylenzyme complex of a class A β-lactamase, SHV-1, that is potently inhibited by carbapenems.[24] Structures are also available for imipenem complexes of TEM-1[25,66] and for complexes of the *Mycobacterium tuberculosis* BlaC enzyme with meropenem,[67] doripenem, and ertapenem.[68] Comparison of our data with these structures and with those of other class A enzymes (Figures 6 and 7) identifies several factors that may be important to the carbapenemase activity of SFC-1 and related enzymes.

Environment of the Deacylating Water. The most important differences concern the environment of the deacylating water (DW; Figures 3 and 6). With respect to carbapenem-inhibited enzymes, the process of productive deacylation of the acylenzyme intermediate is most likely greatly accelerated in class A carbapenemases, consistent with the large differences in carbapenem k_{cat} values between, e.g., SFC-1 (meropenem k_{cat} = 6.5 s^{-1})[39] and BlaC (meropenem k_{cat} = 0.08 min^{-1}).[67] Structural comparisons reveal that the interactions made by the deacylating water molecule differ between SFC-1 and carbapenem-inhibited class A enzymes such as TEM-1, SHV-1 and BlaC (Figure 6). Notably, in carbapenem complexes of these enzymes in the Δ^2-pyrroline tautomer (SHV-1:meropenem,[24] TEM-1:imipenem[25] and BlaC:ertapenem[68]) the deacylating water hydrogen bonds to Glu166 and Asn170 and to the C8 hydroxyl of the carbapenem 6α-1R-hydroxyethyl group. A strong hydrogen bond to the carbapenem C8 hydroxyl has been proposed to reduce the nucleophilicity of the deacylating water in the TEM-1:imipenem[25] and SHV-1:meropenem[24] complexes and thus prolong the lifetimes of these acylenzyme species.

In the SFC-1 Michaelis complex structure (Ser70 Ala mutant; Figure 3A), the deacylating water molecule makes a similar strong hydrogen bond to the C8 hydroxyl group of bound meropenem. However, in the SFC-1 acylenzyme (Glu166 Ala) complex, the meropenem 6α-1R-hydroxyethyl group is rotated such that the interaction with the deacylating water is lost, while that with Asn132 is retained (Figures 3B and 6A). Importantly, our MD simulations (Figures 4 and 5; SI Figures S4 and S5) suggest that this orientation of the meropenem 6α-1R-hydroxyethyl group, as observed crystallographically in the acylenzyme complex of the Glu166 Ala mutant enzyme, is also adopted by the wild-type acylenzyme (and Michaelis complex). These results give us confidence that

dx.doi.org/10.1021/ja304460j | J. Am. Chem. Soc. 2012, 134, 18275−18285

our crystal structure, obtained with a deacylation-deficient mutant, reflects the disposition of bound substrate in the wild-type active site. We conclude that in SFC-1 the reactivity of the deacylating water molecule is maintained by the lack of a hydrogen-bonding interaction with the meropenem C8 hydroxyl group when the 6α-1R-hydroxyethyl substituent is in its favored orientation.

Binding and Tautomerization of the Carbapenem Acylenzyme. Carbapenem inhibition of class A β-lactamases has been associated with tautomerization of the acylenzyme between the Δ^2- (Scheme 1; **3**) and the more hydrolytically inert Δ^1- (Scheme 1; **5**) pyrroline forms. The low activity of the Δ^1-pyrroline tautomer has been ascribed to conformational changes in the active site,[28] or to reorientation of the 6α-1R-hydroxyethyl group of bound carbapenem to permit hydrogen bonding to Glu166, reducing its basicity and consequently deactivating the deacylating water molecule.[68] In enzymes such as TEM-1, acylenzyme tautomerization is proposed to be facilitated by donation of a proton from the conserved Arg244 (or a coordinated water molecule; TW, Figure 6C,D) to the C3 position of bound carbapenem. The importance of this process is shown by the failure of imipenem to inhibit TEM-1 when Arg244 is mutated.[26]

Impaired deacylation has also been associated with conformers of carbapenem acylenzymes in which the carbonyl group is bound outside the oxyanion hole. These have been described for SHV-1 (Figure 6C), TEM-1 (Figure 6D), and CTX-M-9.[27] As the oxyanion hole is expected to promote deacylation by polarizing the carbonyl bond for attack by the deacylating water and by stabilizing the resulting tetrahedral transition state, deacylation may be impaired in conformations where these interactions are disrupted. Raman spectroscopy[28] (SHV-1) and MD[27] (CTX-M-9) studies further associate such states with the Δ^1-pyrroline tautomer, although crystal structures of TEM-1 and SHV-1 complexes show carbapenem acylenzymes in the Δ^2-pyrroline form with their carbonyl groups outside the oxyanion hole.

Consistent with the strong carbapenemase activity of SFC-1, our crystal structure of the meropenem acylenzyme complex provides no evidence for tautomerization of bound meropenem and no evidence for conformers with the carbonyl group positioned outside the oxyanion hole. As has been noted for other carbapenem-hydrolyzing class A β-lactamases, SFC-1 lacks Arg244 (or an equivalent such as Arg276 as present in the CTX-M enzymes[27]) and instead uses Thr235 and Th237 to provide hydrogen bonds to the carbapenem C2 carboxylate (Figures 3 and 6A). While this mode of carbapenem binding might be thought to disfavor carbapenem tautomerization, it closely resembles that adopted by *M. tuberculosis* BlaC (Figure 6B), an enzyme in which tautomerization of bound carbapenems has been clearly demonstrated. However, in BlaC the acylenzyme carbonyl groups of both tautomers are retained in the oxyanion hole. It is proposed that interaction of the carbapenem C2 carboxylate with Thr235 and Thr237 (see above) prevents the rotation of the BlaC acylenzyme carbonyl that is observed in the SHV-1 and TEM-1 enzymes.[68]

Although the comparison with SFC-1 is complicated by the absence of Asn132 in BlaC (where it is replaced by Gly, Figure 6C, see below), the similarity between the modes of carbapenem binding in the two enzymes, which nevertheless differ by more than 3 orders of magnitude in their hydrolytic activity against, e.g., meropenem (see above), permits two conclusions to be drawn. First, binding of the C2 carboxylate to a pair of Thr residues, in place of the Arg more usually found in class A β-lactamases, does not prevent tautomerization of bound carbapenems. Second, retention of the carbapenem acylenzyme carbonyl group within the oxyanion hole is not in itself sufficient for efficient deacylation, while inhibition of class A β-lactamases does not require displacement of the carbonyl oxygen from the oxyanion hole. Taken together, structural comparisons indicate that the carbapenemase activity of SFC-1, and related enzymes, arises primarily from more efficient deacylation of the acylenzyme, rather than from prevention of its rearrangement into unproductive conformations.

Environment of the Carbapenem 6α-1R-Hydroxyethyl Group. Our data indicate that the carbapenemase activity of SFC-1 (and by implication of related class A β-lactamases such as KPC) arises from an altered mode of carbapenem binding, specifically of the 6α-1R-hydroxyethyl group, that preserves the activity of the deacylating water by preventing its interaction with the C8 hydroxyl group while retaining that with Asn132. A central question is then how the active site of SFC-1 enables bound carbapenem to be oriented in this fashion, when those of many other class A β-lactamases do not. As described above, comparison of the active sites of carbapenem-hydrolyzing and carbapenem-inhibited class A β-lactamases does not reveal gross structural differences.[30,35] However, close inspection of the active sites of carbapenem-hydrolyzing class A β-lactamases (SFC-1, KPC-2, NMC-A, SME-1), in comparison with those of carbapenem-inhibited enzymes (TEM-1, SHV-1, CTX-M, BlaC) reveals that the positions of the conserved amino acids differ between the two groups of enzymes (Figure 7). Residues involved include the nucleophilic serine, Ser70, Ser130 (proton donor to the β-lactam nitrogen and hydrogen bonding partner of the carbapenem C2 carboxylate group), Asn132 (hydrogen bonding partner of the carbapenem 6α-1R-hydroxyethyl

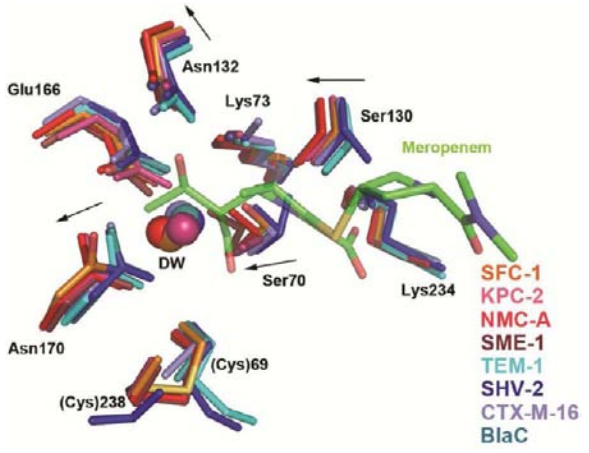

Figure 7. Active sites of Class A β-lactamases. Superposition of active sites of carbapenem-hydrolyzing (wild-type SFC-1 (PDB 4EQI), KPC-2 (PDB 20V5[30]), SME-1 (1DY6[31]), NMC-A (1BUE[29])) and carbapenem-inhibited (TEM-1 (1ZG4[71]), SHV-2 (1N9B[72]), CTX-M-16 (1YLW[73]), BlaC (2GDN[23])) enzymes. Cα atoms are color-coded as shown, carbapenem-hydrolyzing enzymes in red and carbapenem-inhibited enzymes in blue palette. meropenem acylenzyme, as bound in the SFC-1 Glu166 Ala acylenzyme complex structure, is shown with Cα atoms in green. Arrows denote shifts in positions of labeled residues in carbapanem-hydrolyzing enzymes. Superpositions were performed using SSM Superpose[69] to align the complete chains. Cα rmsds are provided in Table S3.

dx.doi.org/10.1021/ja304460j | J. Am. Chem. Soc. 2012, 134, 18275−18285

group), and Asn170 (hydrogen bonds to the deacylating water molecule).

In class A carbapenemases, the Ser70 side chain is shifted, by up to 1 Å, to a less buried position in the active site than is the case in carbapenem-inhibited enzymes. This difference arises from a distinct conformation of the protein backbone at this position, possibly as a result of the constraints imposed by the Cys69−Cys238 disulfide bridge. Furthermore, the side chains of Ser130, Asn132 and Asn170 are in the carbapenemases displaced to more buried positions than in other class A β-lactamases. Superpositions (SSM Superpose;[69] Figure 7) indicate typical differences of 0.85 Å, 0.79 Å, and 1.13 Å in the respective backbone (Cα) and 0.84 Å (Cβ), 0.94 Å (Cγ), and 1.24 Å (Cγ) in the side chain positions for these three residues (values given are from comparison of the SHV-2 and NMC-A structures). Our structures suggest that these changes enlarge the active site sufficiently to prevent steric clashes between Asn170 and the C9 methyl of bound carbapenem when the 6α-1R-hydroxyethyl group rotates to the orientation observed in the SFC-1 acylenzyme crystal structure. (Comparison of active site volumes using CASTp[70] (Table S3) shows an increase from a typical value of c. 110 Å^3 for a carbapenem-inhibited to c. 180 Å^3 for a carbapenem-hydrolyzing enzyme.) Our MD simulations indicate that this orientation, in which the Meropenem C8 hydroxyl hydrogen bonds to SFC-1 Asn132 Nδ2, but not to the deacylating water, is favored in both the Michaelis and acylenzyme complexes.

Our results indicate that Asn132 makes hydrogen bonds to bound substrate that, by stabilizing a conformation where the hydroxyethyl group is not interacting with the deacylating water, are key to carbapenemase activity. This conclusion is also supported by the structure of *M. tuberculosis* BlaC. As described above, the BlaC active site closely resembles that of SFC-1, but BlaC is inhibited by carbapenems and turns these substrates over at rates several orders of magnitude slower than SFC-1 or similar enzymes. Unusually for class A β-lactamases, BlaC lacks Asn132 and features Gly at this position. Thus, the interaction between the C8 hydroxyl of bound carbapenems and the Asn132 side chain, as observed in our SFC-1 structure (Figure 6A) is impossible, and consequently in BlaC carbapenem complexes, the carbapenem 6α-1R-hydroxyethyl group interacts with the deacylating water (Δ^2-pyrroline; Figure 6B) or adjacent amino acids (Glu166, Lys73; Δ^1-pyrroline). In other carbapenem-inhibited class A β-lactamases, Asn132 is present and is hydrogen bonded to the 6α-1R-hydroxyethyl group of bound carbapenems (Figure 6C,D). However, in these cases the more restricted active site orients bound carbapenem to prevent the rotation of the 6α-1R-hydroxyethyl group to the conformation observed in SFC-1 (Figure 6A), favoring interaction of the C8 hydroxyl with the deacylating water molecule.

Repositioning of Asn132, compared to its position in carbapenem-inhibited enzymes, has been noted in previous structures of class A carbapenemases. In the majority of class A β-lactamases, Asn132 has been proposed to promote β-lactam hydrolysis by hydrogen bonding to the oxygen atoms of the 6β- or 7β-amido groups of penicillin or cephalosporin substrates, respectively.[74] However, the α-, rather than β-, stereochemistry of the carbapenem 6−1R-hydroxyethyl substituent creates a steric clash on carbapenem binding to, e.g., the TEM-1 enzyme[25] that is alleviated when this residue is mutated.[66] Importantly, however, Asn132 mutations alone are not sufficient to confer carbapenemase activity on enzymes such as TEM-1. In class A carbapenemases such as NMC-A repositioning of Asn132 has been proposed to contribute to an enlarged active site that is able to accommodate the carbapenem 6α-1R-hydroxyethyl substituent.[29] This conclusion is supported by the structure of the NMC-A enzyme in complex with a 6α-hydroxypropyl penicillinate inhibitor,[75] which features hydrogen bonds between the inhibitor hydroxyl group and both Asn132 and the deacylating water. In the KPC-2 carbapenemase, it has been proposed that movement of key residues, including Ser70, Ser130, Asn132 and Asn170, from their positions in carbapenem-inhibited enzymes enlarges the active site sufficiently to permit carbapenems to bind in productive conformations.[30] The present work expands on these studies by providing the first structural description of the interactions between a carbapenem substrate and a class A carbapenemase.

Concluding Remarks. In summary, the data we present here reveal for the first time the interactions between a carbapenem antibiotic and a class A β-lactamase with potent activity against these clinically highly significant drugs. Our crystal structures and MD simulations show a mode of carbapenem binding to SFC-1 in which the C8 hydroxyl of the carbapenem 6α-1R-hydroxyethyl group interacts with Asn132, but does not hydrogen bond to the water molecule responsible for deacylation. Such interactions reduce the nucleophilicity of the deacylating water molecule in other class A enzymes. Subtle alterations to the locations of residues including Ser70 and Asn132 in the class A carbapenemase active site may permit this distinctive mode of carbapenem binding by relieving steric clashes that would otherwise constrain the orientation of the 6α-1R-hydroxyethyl group. In light of the continuing dissemination of class A carbapenemases, in particular, KPC, in bacterial strains responsible for healthcare-associated infection, and the reduced susceptibility of such enzymes to clinically available β-lactamase inhibitors, new strategies for countering their activity are required. Our structures suggest that optimizing the interactions of enzyme-bound β-lactams with the deacylating water may represent one such strategy.

■ ASSOCIATED CONTENT

Ⓢ Supporting Information

Additional Materials and Methods; description of the wild-type SFC-1 crystal structure; tables of oligonucleotide primers used for site-directed mutagenesis (Table S1), crystallographic statistics (Table S2), and details of structural comparisons (Table S3); figures showing overall structure of SFC-1 (Figure S1), comparison with other class A β-lactamase crystal structures (Figure S2), active site of the unliganded (wild-type) enzyme (Figure S3), time-dependence of Cα rmsds from starting (crystal) structures for MD simulations (Figure S4); overlays of complex crystal structures with models derived from clustering analysis of MD runs (Figure S5). Complete reference 58. This material is available free of charge via the Internet at http://pubs.acs.org.

■ AUTHOR INFORMATION

Corresponding Author

*E-mail: maria.fonseca@ibmc.up.pt; Adrian.Mulholland@bristol.ac.uk; Jim.Spencer@bristol.ac.uk.

Present Address

[#]Instituto de Biologia Molecular e Celular, Universidade do Porto, Rua do Campo Alegre, 823, 4150−180 Porto − Portugal.

Notes

The authors declare no competing financial interest.

■ ACKNOWLEDGMENTS

This work was supported by CESAM (Centre for Environmental and Marine Studies), University of Aveiro, Portugal; and by the Fundação para a Ciência e a Tecnologia, Portugal (PhD grant BD/30490/2006 to F.F.). E.I.C., M.W.K., and A.J.M. thank the U.K. Engineering and Physical Science Research Council (grant number EP/G007705/1) for support. A.J.M. is an engineering and Physical Science Research Council Leadership Fellow. This work was carried out with the support of the Diamond Light Source. U.K. Northwest Structural Genomics Centre (NWSGC) MAD10 beamline at SRS (U.K.) was funded by the U.K. Biotechnology and Biological Sciences Research Council (grant numbers 719/B15474 and 719/REI20571) and a North West Development Agency project award (N0002170). We thank Mark Ellis (SRS) and the staff of Diamond Beamlines IO2 and IO3 for their assistance with data collection. Coordinates and structure factors for the crystal structures described here have been deposited in the Protein Data Bank (accession codes: 4EQI for wild-type SFC-1; 4EUZ for the S70A:meropenem complex and 4EV4 for the E166A:meropenem complex, respectively).

■ REFERENCES

(1) Nicolau, D. P. *Expert Opinion on Pharmacotherapy* **2008**, *9*, 23.
(2) Papp-Wallace, K. M.; Endimiani, A.; Taracila, M. A.; Bonomo, R. A. *Antimicrob. Agents Chemother.* **2011**, *55*, 4943.
(3) Masterton, R. G. *Int. J. Antimicrob. Agents* **2009**, *33*, 105.
(4) Fisher, J. F.; Meroueh, S. O.; Mobashery, S. *Chem. Rev.* **2005**, *105*, 395.
(5) Pfeifer, Y.; Cullik, A.; Witte, W. *Int. J. Med. Microbiol.* **2010**, *300*, 371.
(6) Walsh, T. R. *Int. J. Antimicrob. Agents* **2010**, *36*, S8.
(7) Ambler, R. P. *Philos. Trans. R. Soc. London, Ser. B: Biol. Sci.* **1980**, *289*, 321.
(8) Patel, G.; Bonomo, R. A. *Expert Rev. Anti Infect. Ther.* **2011**, *9*, 555.
(9) Rasmussen, B. A.; Bush, K.; Keeney, D.; Yang, Y.; Hare, R.; O'Gara, C.; Medeiros, A. A. *Antimicrob. Agents Chemother.* **1996**, *40*, 2080.
(10) Naas, T.; Nordmann, P. *Proc. Natl. Acad. Sci. U. S. A.* **1994**, *91*, 7693.
(11) Mariotte-Boyer, S.; Nicolas-Chanoine, M. H.; Labia, R. *FEMS Microbiol. Lett.* **1996**, *143*, 29.
(12) Naas, T.; Vandel, L.; Sougakoff, W.; Livermore, D. M.; Nordmann, P. *Antimicrob. Agents Chemother.* **1994**, *38*, 1262.
(13) Yigit, H.; Queenan, A. M.; Anderson, G. J.; Domenech-Sanchez, A.; Biddle, J. W.; Steward, C. D.; Alberti, S.; Bush, K.; Tenover, F. C. *Antimicrob. Agents Chemother.* **2001**, *45*, 1151.
(14) Henriques, I.; Moura, A.; Alves, A.; M.J., S.; Correia, A. *Antimicrob. Agents Chemother.* **2004**, *48*, 2321.
(15) Bae, I. K.; Lee, Y. N.; Jeong, S. H.; Hong, S. G.; Lee, J. H.; Lee, S. H.; Kim, H. J.; Youn, H. *Diagn. Microbiol. Infect. Dis.* **2007**, *58*, 465.
(16) Bonnin, R. A.; Nordmann, P.; Potron, A.; Lecuyer, H.; Zahar, J. R.; Poirel, L. *Antimicrob. Agents Chemother.* **2011**, *55*, 349.
(17) Kotsakis, S. D.; Miriagou, V.; Tzelepi, E.; Tzouvelekis, L. S. *Antimicrob. Agents Chemother.* **2010**, *54*, 4864.
(18) Poirel, L.; Weldhagen, G. F.; Naas, T.; De Champs, C.; Dove, M. G.; Nordmann, P. *Antimicrob. Agents Chemother.* **2001**, *45*, 2598.
(19) Vourli, S.; Giakkoupi, P.; Miriagou, V.; Tzelepi, E.; Vatopoulos, A. C.; Tzouvelekis, L. S. *FEMS Microbiol. Lett.* **2004**, *234*, 209.
(20) Wachino, J.; Doi, Y.; Yamane, K.; Shibata, N.; Yagi, T.; Kubota, T.; Arakawa, Y. *Antimicrob. Agents Chemother.* **2004**, *48*, 2905.
(21) Nordmann, P.; Cuzon, G.; Naas, T. *Lancet Infect. Dis.* **2009**, *9*, 228.
(22) Perez, F.; Endimiani, A.; Hujer, K. M.; Bonomo, R. A. *Curr. Opin. Pharmacol.* **2007**, *7*, 459.
(23) Wang, F.; Cassidy, C.; Sacchettini, J. C. *Antimicrob. Agents Chemother.* **2006**, *50*, 2762.
(24) Nukaga, M.; Bethel, C. R.; Thomson, J. M.; Hujer, A. M.; Distler, A.; Anderson, V. E.; Knox, J. R.; Bonomo, R. A. *J. Am. Chem. Soc.* **2008**, *130*, 12656.
(25) Maveyraud, L.; Mourey, L.; Kotra, L. P.; Pedelacq, J. D.; Guillet, V.; Mobashery, S.; Samama, J. P. *J. Am. Chem. Soc.* **1998**, *120*, 9748.
(26) Zafaralla, G.; Mobashery, S. *J. Am. Chem. Soc.* **1992**, *114*, 1505.
(27) Bethel, C. R.; Taracila, M.; Shyr, T.; Thomson, J. M.; Distler, A. M.; Hujer, K. M.; Hujer, A. M.; Endimiani, A.; Papp-Wallace, K.; Bonnet, R.; Bonomo, R. A. *Antimicrob. Agents Chemother.* **2011**, *55*, 3465.
(28) Kalp, M.; Carey, P. R. *Biochemistry* **2008**, *47*, 11830.
(29) Swaren, P.; Maveyraud, L.; Raquet, X.; Cabantous, S.; Duez, C.; Pedelacq, J. D.; Mariotte-Boyer, S.; Mourey, L.; Labia, R.; Nicolas-Chanoine, M. H.; Nordmann, P.; Frere, J. M.; Samama, J. P. *J. Biol. Chem.* **1998**, *273*, 26714.
(30) Ke, W.; Bethel, C. R.; Thomson, J. M.; Bonomo, R. A.; van den Akker, F. *Biochemistry* **2007**, *46*, 5732.
(31) Sougakoff, W.; L'Hermite, G.; Pernot, L.; Naas, T.; Guillet, V.; Nordmann, P.; Jarlier, V.; Delettre, J. *Acta Crystallogr., Sect. D: Biol. Crystallogr.* **2002**, *58*, 267.
(32) Petrella, S.; Ziental-Gelus, N.; Mayer, C.; Renard, M.; Jarlier, V.; Sougakoff, W. *Antimicrob. Agents Chemother.* **2008**, *52*, 3725.
(33) Frase, H.; Shi, Q.; Testero, S. A.; Mobashery, S.; Vakulenko, S. B. *J. Biol. Chem.* **2009**, *284*, 29509.
(34) Majiduddin, F. K.; Palzkill, T. *Antimicrob. Agents Chemother.* **2003**, *47*, 1062.
(35) Majiduddin, F. K.; Palzkill, T. *Antimicrob. Agents Chemother.* **2005**, *49*, 3421.
(36) Papp-Wallace, K. M.; Taracila, M.; Hornick, J. M.; Hujer, A. M.; Hujer, K. M.; Distler, A. M.; Endimiani, A.; Bonomo, R. A. *Antimicrob. Agents Chemother.* **2010**, *54*, 2867.
(37) Papp-Wallace, K. M.; Taracila, M.; Wallace, C. J.; Hujer, K. M.; Bethel, C. R.; Hornick, J. M.; Bonomo, R. A. *Protein Sci.* **2010**, *19*, 1714.
(38) Pfyffer, G. E. *Eur. J. Clin. Microbiol. Infect. Dis.* **1992**, *11*, 199.
(39) Fonseca, F.; Sarmento, A. C.; Henriques, I.; Samyn, B.; van Beeumen, J.; Domingues, P.; Domingues, M. R.; Saavedra, M. J.; Correia, A. *Antimicrob. Agents Chemother.* **2007**, *51*, 4512.
(40) Saavedra, M. J.; Peixe, L.; Sousa, J. C.; Henriques, I.; Alves, A.; Correia, A. *Antimicrob. Agents Chemother.* **2003**, *47*, 2330.
(41) Fonseca, F.; Arthur, C. J.; Bromley, E. H.; Samyn, B.; Moerman, P.; Saavedra, M. J.; Correia, A.; Spencer, J. *Antimicrob. Agents Chemother.* **2011**, *55*, 5392.
(42) Fonseca, F.; Bromley, E. H.; Saavedra, M. J.; Correia, A.; Spencer, J. *J. Mol. Biol.* **2011**, *411*, 951.
(43) Papp-Wallace, K. M.; Bethel, C. R.; Distler, A. M.; Kasuboski, C.; Taracila, M.; Bonomo, R. A. *Antimicrob. Agents Chemother.* **2010**, *54*, 890.
(44) Yigit, H.; Queenan, A. M.; Rasheed, J. K.; Biddle, J. W.; Domenech-Sanchez, A.; Alberti, S.; Bush, K.; Tenover, F. C. *Antimicrob. Agents Chemother.* **2003**, *47*, 3881.
(45) Strynadka, N. C.; Adachi, H.; Jensen, S. E.; Johns, K.; Sielecki, A.; Betzel, C.; Sutoh, K.; James, M. N. *Nature* **1992**, *359*, 700.
(46) Adachi, H.; Ohta, T.; Matsuzawa, H. *J. Biol. Chem.* **1991**, *266*, 3186.
(47) Hermann, J. C.; Ridder, L.; Höltje, L. D.; Mulholland, A. J. *Org. Biomol. Chem.* **2006**, *4*, 206.
(48) Otwinowski, Z.; Minor, W. *Methods Enzymol.* **1997**, *276*, 307.

(49) Leslie, A. G. W. *Joint CCP4 + ESF-EAMCB Newsletter on Protein Crystallography* **1992**, *26*, 27.
(50) Evans, P. R. *Acta Crystallogr., Sect. D: Biol. Crystallogr.* **2005**, *62*, 72.
(51) McCoy, A. J.; Grosse-Kunstleve, R. W.; Adams, P. D.; Winn, M. D.; Storoni, L. C.; Read, R. J. *J. Appl. Crystallogr.* **2007**, *40*, 658.
(52) Emsley, P.; Lohkamp, B.; Scott, W. G.; Cowtan, K. *Acta Crystallogr., Sect. D: Biol. Crystallogr.* **2010**, *66*, 486.
(53) Murshudov, G. N.; Vagin, A. A.; Dodson, E. J. *Acta Crystallogr., Sect. D: Biol. Crystallogr.* **1997**, *53*, 240.
(54) Sheldrick, G. M. *Acta Crystallogr., Sect. A* **2008**, *64*, 112.
(55) Chen, V. B.; Arendall, W. B., 3rd; Headd, J. J.; Keedy, D. A.; Immormino, R. M.; Kapral, G. J.; Murray, L. W.; Richardson, J. S.; Richardson, D. C. *Acta Crystallogr., Sect. D: Biol. Crystallogr.* **2010**, *66*, 12.
(56) Laskowski, R. A.; MacArthur, M. W.; Moss, D. S.; Thornton, J. M. *J. Appl. Crystallogr.* **1993**, *26*, 283.
(57) Case, D. A.; Darden, T. A.; Cheatham III, T. E.; Simmerling, C. L.; Wang, J.; Duke, R. E.; Luo, R.; Walker, R. C.; Zhang, W.; Merz, K. M.; Roberts, B.; Wang, B.; Hayik, S.; Roitberg, A.; Seabra, G.; Kolossváry, I.; Wong, K. F.; Paesani, F.; Vanicek, J.; Liu, J.; Wu, X.; Brozell, S. R.; Steinbrecher, T.; Gohlke, H.; Cai, Q.; Ye, X.; Wang, J.; Hsieh, M.-J.; Cui, G.; Roe, D. R.; Mathews, D. H.; Seetin, M. G.; Sagui, C.; Babin, V.; Luchko, T.; Gusarov, S.; Kovalenko, A.; Kollman, P. A.; *AMBER 11*; University of California, San Francisco, 2010.
(58) Hornak, V.; Abel, R.; Okur, A.; Strockbine, B.; Roitberg, A.; Simmerling, C. *Proteins* **2006**, *65*, 712.
(59) Wang, J.; Wolf, R. M.; Caldwell, J. W.; Kollman, P. A.; Case, D. A. *J. Comput. Chem.* **2004**, *25*, 1157.
(60) Leyssene, D.; Delmas, J.; Robin, F.; Cougnoux, A.; Gibold, L.; Bonnet, R. *Antimicrob. Agents Chemother.* **2011**, *55*, 5660.
(61) Beadle, B. M.; Trehan, I.; Focia, P. J.; Shoichet, B. K. *Structure* **2002**, *10*, 413.
(62) Shimamura, T.; Ibuka, A.; Fushinobu, S.; Wakagi, T.; Ishiguro, M.; Ishii, Y.; Matsuzawa, H. *J. Biol. Chem.* **2002**, *277*, 46601.
(63) Tremblay, L. W.; Xu, H.; Blanchard, J. S. *Biochemistry* **2010**, *49*, 9685.
(64) Hermann, J. C.; Hensen, C.; Ridder, L.; Mulholland, A. J.; Höltje, L. D. *J. Am. Chem. Soc.* **2005**, *127*, 4454.
(65) Hermann, J. C.; Ridder, L.; Mulholland, A. J.; Höltje, L. D. *J. Am. Chem. Soc.* **2003**, *125*, 9590.
(66) Wang, X.; Minasov, G.; Shoichet, B. K. *Proteins* **2002**, *47*, 86.
(67) Hugonnet, J. E.; Tremblay, L. W.; Boshoff, H. I.; Barry, C. E., 3rd; Blanchard, J. S. *Science* **2009**, *323*, 1215.
(68) Tremblay, L. W.; Fan, F.; Blanchard, J. S. *Biochemistry* **2010**, *49*, 3766.
(69) Krissinel, E.; Henrick, K. *Acta Crystallogr., Sect. D: Biol. Crystallogr.* **2004**, *60*, 2256.
(70) Dundas, J.; Ouyang, Z.; Tseng, J.; Binkowski, A.; Turpaz, Y.; Liang, J. *Nucleic Acids Res.* **2006**, *34*, W116.
(71) Stec, B.; Holtz, K. M.; Wojciechowski, C. L.; Kantrowitz, E. R. *Acta Crystallogr., Sect. D: Biol. Crystallogr.* **2005**, *61*, 1072.
(72) Nukaga, M.; Mayama, K.; Hujer, A. M.; Bonomo, R. A.; Knox, J. R. *J. Mol. Biol.* **2003**, *328*, 289.
(73) Chen, Y.; Bonnet, R.; Shoichet, B. K. *J. Am. Chem. Soc.* **2007**, *129*, 5378.
(74) Fonze, E.; Vanhove, M.; Dive, G.; Sauvage, E.; Frere, J. M.; Charlier, P. *Biochemistry* **2002**, *41*, 1877.
(75) Mourey, L.; Miyashita, K.; Swaren, P.; Bulychev, A.; Samama, J. P.; Mobashery, S. *J. Am. Chem. Soc.* **1998**, *120*, 9382.